Available online at www.sciencedirect.com
ScienceDirect
Biochemical and Biophysical Research Communications 348 (2006) 301–309
BBRC
www.elsevier.com/locate/ybbrc

Properties of ion channels in rabbit mesenchymal stem cells from bone marrow

Xiu-Ling Deng, Hai-Ying Sun, Chu-Pak Lau, Gui-Rong Li *

Department of Medicine and Research Centre of Heart, Brain, Hormone and Healthy Aging, Li Ka Shing Faculty of Medicine, The University of Hong Kong, Pokfulam, Hong Kong SAR, China

Received 7 July 2006
Available online 20 July 2006

Abstract

The present study was designed to investigate properties of ion channels in undifferentiated rabbit mesenchymal stem cells (MSCs) from bone marrow using whole-cell patch-clamp and RT-PCR techniques. It was found that three types of outward currents were present in rabbit MSCs, including an inward rectifier K^+ current (I_{Kir}), a noise-like Ca^{2+}-activated K^+ current (I_{KCa}) co-present with delayed rectifier K^+ current (IK_{DR}). I_{Kir} was inhibited by Ba^{2+}, while I_{KCa} was inhibited by paxilline (a blocker of big conductance I_{KCa} channels) and clotrimazole (an inhibitor of intermediate conductance I_{KCa} channels). IK_{DR} exhibited a slow inactivation, "U-shaped" voltage-dependent inactivation, and slow recovery from inactivation, and the current was inhibited by tetraethylammonium or 4-aminopyridine. RT-PCR revealed the molecular identities for the functional ionic currents, including Kir1.1 (possibly responsible for I_{Kir}), KCa1.1 and KCa3.1 (possibly responsible for I_{KCa}), and Kv1.2, Kv2.1, and Kv2.2 (possibly responsible for IK_{DR}). These results demonstrate for the first time that three types of functional ion channel currents (i.e., I_{Kir}, I_{KCa}, and IK_{DR}) are present in rabbit MSCs from bone marrow.

Keywords: Rabbit; Mesenchymal stem cells; Ion channels; Delayed rectifier potassium current; Calcium-activated potassium current; Inward rectifier potassium current

Mesenchymal stem cells (MSCs) from bone marrow have been recently cultured and expanded *in vitro* from different species (e.g., mice, rats, and humans). MSCs exhibited multilineage potential [1–4] to incorporate into a variety of tissues, including bone, cartilage, muscle, lung, and spleen, by in vivo transplantation [2,3,5,6]. MSCs were also found to form other kinds of cells *in vitro*, e.g., hepatocytes, cardiomyocytes, and neuronal cells [1,2,7]. In addition, transplantation of MSCs to the infarcted myocardium significantly improved heart function in experimental studies [8–10]. Therefore, it is believed that MSCs are an ideal cell source for myocardioregeneration [1,7,11,12]. However, limited information is available in the literature regarding cellular electrophysiology in MSCs. A few of recent reports from our and other two laboratories demonstrated that multiple ion channel currents were present in human [13–15] and rat [16] MSCs, and the ion channel expression was species-dependent. The present study was designed to characterize ion channels in rabbit undifferentiated MSCs from bone marrow. We found that the types of ion channels in rabbit MSCs were different from those in human MSCs and/or rat MSCs.

Materials and methods

Isolation and culture of rabbit MSCs. Rabbit MSCs were obtained from bone marrow of New Zealand White rabbits (2–3 kg, either sex) by the Guideline for Animal Care and Use Committee for Teaching and Research of University of Hong Kong with a modified procedure as previously described [17,18]. Briefly, after the animal was anesthetized with ketamine hydrochloride and xylazine (60: 6 mg/kg, iv), bone marrow was aspirated from the iliac crest of rabbit under sterile con-

* Corresponding author. Fax: +852 2855 9730.
E-mail address: grli@hkucc.hku.hk (G.-R. Li).

0006-291X/$ - see front matter © 2006 Elsevier Inc. All rights reserved.
doi:10.1016/j.bbrc.2006.07.054

ditions. The aspirated marrow was mixed and dispersed with the complete culture medium consisting of Iscove's modified Dulbecco's medium (IMDM; Sigma–Aldrich Chemicals, St. Louis, MO), 10% fetal bovine serum (FBS, Invitrogen, Hong Kong), and antibiotics (100 U/ml penicillin G, 100 μg/ml streptomycin sulfate, and 0.25 μg/ml amphotericin B; Invitrogen). The collected bone marrow was centrifuged at 1000 rpm for 10 min. After the suspension was removed, the pellet was re-suspended in 2.5 ml of the complete culture medium, and carefully layered over 10 ml of Percoll cushion, and centrifuged at 14,000 rpm for 12 min at 8 °C. Cells were collected at top 60% of the gradient and washed twice with the complete culture medium. The cells were seeded into a 25 cm^2 tissue culture flask and incubated at 37 °C in a humidified atmosphere with 5% CO_2. Non-adherent cells were removed after 24 h, and MSCs adhered to the flask bottom gradually proliferated to form colonies between 5 and 7 days. Once the colonies reached 80–90% confluence, they were detached with trypsin/EDTA, centrifuged at 1000 rpm for 8 min, and suspended in medium for continuous culture. For ionic current study, cells (from 1 to 4 passages) were transferred to a cell chamber mounted on the stage of the inverted microscope (Leica, DM IL) for a 15–20 min and allowed to attach to the bottom of the cell chamber. Subsequently, the cells were superfused with normal Tyrode solution (1.5 ml/min).

Osteogenic and adipogenic differentiation were conducted in rabbit MSCs (passages 3–4) as described previously [16]. Staining of alkaline phosphatase aggregates and examination of alkaline phosphatase activity, and the oil red O staining for the lipid accumulation indicated that rabbit MSCs exhibited the potency to differentiate into bone cells or adipocytes *in vitro* (data not shown).

Electrophysiology. The rabbit MSCs from passages 1 to 4 were used for ionic current study with whole-cell patch-clamp technique as described previously [14,16]. Borosilicate glass electrodes (1.2 mm OD) were pulled with a Brown–Flaming puller (Model P-97, Sutter Instrument Co., Novato, CA), and had tip resistances of 2–3 MΩ, when filled with pipette solution. The tip potentials were compensated before the pipette touched the cell. After a gigaohm-seal was obtained by negative suction, the cell membrane was ruptured by gentle suction to establish whole-cell configuration. Data were acquired with an EPC9 amplifier (Heka, Lambrecht, Germany). Membrane currents were low-pass filtered at 5 kHz and stored on the hard disk of an IBM compatible computer.

Tyrode solution contained (mM): 136 NaCl, 5.4 KCl, 1.0 $MgCl_2$, 1.8 $CaCl_2$, 0.33 NaH_2PO_4, 10 glucose, and 10 Hepes; pH adjusted to 7.4 with NaOH. The pipette solution contained (mM): 20 KCl, 110 K-aspartate, 1.0 $MgCl_2$, 10 Hepes, 0.05 EGTA, 0.1 GTP, 5.0 Na_2-phosphocreatine, and 5.0 Mg_2-ATP; pH adjusted to 7.2 with KOH. The experiments were conducted at room temperature (21–22 °C).

Reverse transcript polymerase chain reaction. Total RNA of rabbit MSCs (from passages 2 to 4) was isolated using TRIzol method (Invitrogen) and then treated with DNase I (Invitrogen). Reverse transcription (RT) was performed with RT system (Promega, Madison, WI) protocol in a 20 μl reaction mixture. RNA (1.5 μg) was used in the reaction, and random hexamer primer was used for the initiation of cDNA synthesis. After this RT procedure, the reaction mixture (cDNA) was used for polymerase chain reaction (PCR).

The forward and reverse PCR oligonucleotide primers chosen to amplify the cDNA are listed in Table 1. PCR was performed by a Promega PCR system with Taq polymerase and accompanying buffers as previously described [14,16]. The PCR products were electrophoresed through a 1% agarose gel, and the amplified cDNA bands were visualized by ethidium bromide staining. The bands imaged by Chemi-Genius Bio Imaging System (Syngene, Cambridge, UK) were analyzed via GeneTools software (Syngene).

Data analysis. Non-linear curve-fitting programs (Pulsefit or Sigmaplot, SPSS, Chicago, IL) were used to perform curve-fitting procedures. Results are presented as means ± SEM. Paired and unpaired Student's *t* tests were used as appropriate to evaluate the statistical significance of differences between two group means, and analysis of variance (ANOVA) was used for multiple groups. Values of $P < 0.05$ were considered to indicate statistical significance.

Results

Families of ion channel currents

Families of membrane currents recorded in undifferentiated rabbit MSCs are illustrated in Fig. 1. Two components of ionic currents were activated by voltage protocol as shown in the inset in a representative rabbit MSC (Fig. 1A). One component showed a gradual activating current at potentials from −20 to +30 mV, typical of delayed rectifier K^+ current (IK_{DR}). Another was a rapidly activating current with noisy oscillation at +30 to +60 mV, like Ca^{2+}-activated K^+ current (I_{KCa}). I_{KCa} was co-present with IK_{DR} in 29% of rabbit MSCs (65 out of 228 cells). The typical IK_{DR} was recorded in another rabbit MSC (Fig. 1B), and similar recording was observed in 71% of rabbit MSCs (163 of 228 cells). Fig. 1C demonstrates an inward rectifier K^+ current (I_{Kir}) activated by a hyperpolarization voltage protocol (inset) in another rabbit MSC. I_{Kir} was recorded in 28% of rabbit MSCs (64 out of 228 cells). The rabbit MSCs investigated had membrane potentials between −29 and −71 mV. Mean value of membrane capacitance was 41.15 ± 1.9 pF ($n = 228$).

Blockade of I_{Kir} by Ba^{2+}

It is generally believed that Kir channels are sensitive to inhibition by Ba^{2+}. We therefore determined the effect of Ba^{2+} on I_{Kir} in rabbit MSCs. Fig. 2A shows original traces recorded in a representative cell with the voltage protocol as shown in the inset before and after application of Ba^{2+}. Ba^{2+} at 500 μM substantially reduced I_{Kir}, and the effect recovered upon washout. Fig. 2B displays the *I–V* relationships determined in the absence and presence of 500 μM Ba^{2+} in seven rabbit MSCs. Ba^{2+}-sensitive I_{Kir} exhibits an *I–V* relationship typical inwardly rectifying current.

Ca^{2+}-activated K^+ currents

Three types of I_{KCa} have been described in different types of cells by the use of selective I_{KCa} channel blockers [19–21]. Fig. 3A shows membrane current traces recorded in a representative rabbit MSC in the absence (control) and presence of ion channel blockers. Total current was partially inhibited and the noisy oscillation was reduced by the application of 1 μM paxilline (a blocker of big conductance Ca^{2+}-activated K^+ channels, Sigma–Aldrich). Combination of paxilline with 1 μM clotrimazole (a blocker of intermediate conductance Ca^{2+}-activated K^+ channels) produced an additional inhibition of the membrane currents. The remaining current, most likely IK_{DR}, was suppressed by the co-application of paxilline and clotrimazole with 5 mM 4-aminopyridine (4-AP). Fig. 3B illustrates the *I–V* relationships of membrane currents during control, in the presence of 1 μM paxilline, paxilline plus 1 μM clotrimazole, and paxilline with clotrimazole plus 5 mM 4-

Table 1
Oligonucleotide sequences of primers used for RT-PCR

Name (Accession No.)	Primer sequence (5′–3′)	Fragment size (bp)
Kv1.1 (NM_173095)	Sense: CATGACCACTGTGGGATACG Antisense: ACAGAGTGGGACAGGAGTCG	449
Kv1.2 (NM_012970)	Sense: GAGATGTTTCGGGAGGATGA Antisense: CTCTGTCCCCAGGGTGATAA	450
Kv1.3 (NM_019270)	Sense: ATTGTAGCCATCATCCCTTAT Antisense: AGCCTTCAGTGTCTGTCCC	183
Kv1.4 (NM_012971)	Sense: GCCATCGTATCTGTCCTGGT Antisense: CCTTGGAGTGTCTGGAGAGC	460
Kv1.5 (D45025)	Sense: TGCCCGAGTTCAAGGACG Antisense: GGCGAAGAAACGCACAAGC	224
Kv2.1 (X16476)	Sense: GCTGCAGAGCCTAGACGAGT Antisense: TGCTTTTGAACTTGGTGTCG	452
Kv2.2 (M77482)	Sense: TCGTCCTTTCCACCATTGC Antisense: TTCCCATGGCCAGAAACAG	429
Kv3.1 (NM_012856)	Sense: CCCTCCTTGTCAGTCTCTGC Antisense: CAGACCCAGCTCTCAACCTC	489
Kv3.2 (NM_139217)	Sense: TCCAAAGCGGCTAAAGATG Antisense: CAAAACTCCCAGAGCCAGA	174
Kv4.2 (NM_031730)	Sense: CATGGCCCTGGTGTTCTACT Antisense: GCAAGAAGCCCAGTTCTGAC	473
Kv4.3 (NM_031739)	Sense: GCTGGGTAGCACAGAGAAGG Antisense: GTGTCCAGGCAGAAGAAAGC	498
Kir1.1 (NM017023)	Sense: CAACTGTGCTGGACCTGAAA Antisense: CGCATTCTTGCTGAACGTAA	386
Kir2.1 (NM008425)	Sense: CTCTCCTGGCTGTTCTTTGG Antisense: TGCGGTCAATTCCACTATCA	502
Kir2.2 (NM010603)	Sense: GGGCCTAGACCGTATCTTCC Antisense: AAGGCCAGCTCGTTCTCATA	378
$Ca_V1.2$ (M86621)	Sense: GTCCAGATCCTTGCGACAT Antisense: AGCGAACTCCCAAACCTC	462
$Ca_V3.1$ (AF086827)	Sense: CTGGTCGGTCTACCTCTTCTC Antisense: TACGCCTGCTCACCAAAG	264
$Na_V1.1$ (U35238)	Sense: CTCAGCATTCGTGGTTCATTG Antisense: CACTGTGCATCTTCCCGTTC	253
KCa1.1 (AF135265)	Sense: TGTGGGCTCCATCGAGTA Antisense: GCTTAGCGAGTTCCGTGA	386
KCa3.1 (NM_023021)	Sense: CACGCTGAGATGTTGTGGTT Antisense: CGATGCTGCGGTAAGACG	415
KCa2.3 (AF292389)	Sense: CCAACGCTACCCACAACC Antisense: CGTGCCGTCCAGAAGAAC	457
GAPDH (NM_001001303)	Sense: TCAACGGCACAGTCAAGG Antisense: ACCAGTGGATGCAGGGAT	470

Kv, voltage-gated potassium channel; Kir, inward rectifier potassium channel; $Ca_V1.2$, L-type calcium channel α-2 subunit; $Ca_V3.1$, T-type calcium channel α-1 subunit; $Na_V1.1$, α-subunit of sodium channel; KCa1.1, big conductance calcium-activated potassium channel; KCa3.1, intermediate conductance calcium-activated channel; KCa2.3, small conductance calcium-activated potassium channel SK3; GAPDH, glyceraldehyde-3-phosphate dehydrogenase.

AP. The membrane currents measured at +60 mV were reduced by 29.0 ± 2.9, 52.8 ± 1.4, and $84.1 \pm 4.0\%$ with paxilline, paxillline plus clotrimazole, and paxilline plus clotrimazole and 4-AP, respectively ($n = 6$, $P < 0.01$ vs control), suggesting that big and intermediate conductance I_{KCa} are co-expressed with IK_{DR} in rabbit MSCs.

In addition, we found that the peptide toxins iberiotoxin (an inhibitor of big conductance I_{KCa} channels, 100 nM, $n = 6$) and charybdotoxin (an inhibitor of big and intermediate conductance I_{KCa} channels, 100 nM, $n = 7$) also significantly inhibited the membrane currents ($P < 0.01$). However, apamin (an inhibitor of small conductance I_{KCa}, 100 nM) had no effect on membrane currents in rabbit MSCs ($n = 6$, $P =$ NS). These results indicate that big and intermediate conductance I_{KCa} channels, but not small conductance I_{KCa} channel, are present in rabbit MSCs.

Properties of IK_{DR}

IK_{DR} was studied in rabbit MSCs showing no noise-like current. Fig. 4A shows IK_{DR} traces recorded in a typical experiment in the absence and presence of tetraethylammonium (TEA). IK_{DR} was reversibly suppressed by the application of 10 mM TEA. Concentration–response relationship of TEA effect on IK_{DR} was assessed in nine cells with 0.1, 0.3, 1, 3, and 10 mM TEA, and fitted to

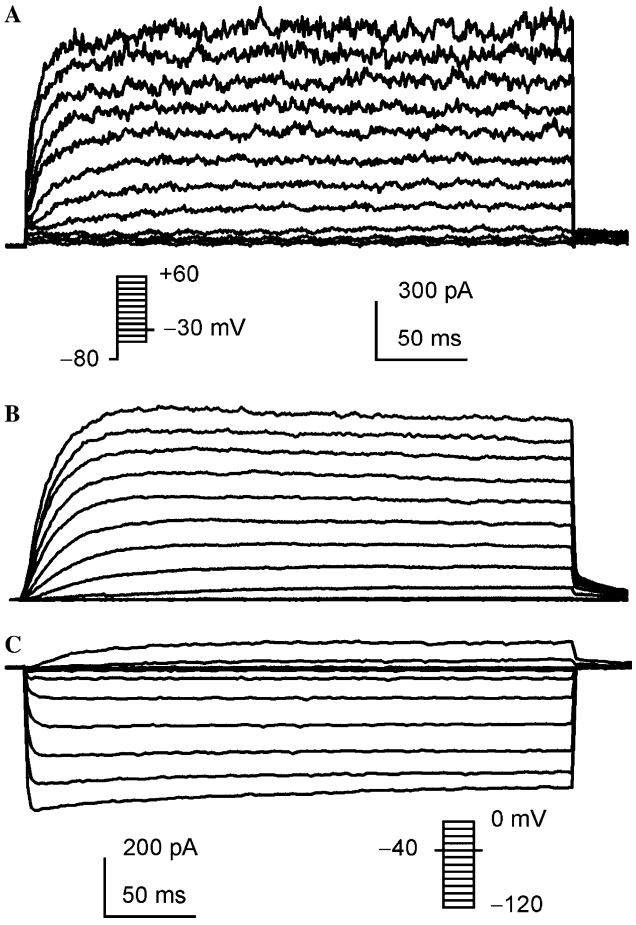

Fig. 1. Families of membrane currents in cultured rabbit MSCs. (A) Membrane currents recorded with 300-ms voltage steps from −80 to between −50 and +60, and then back to −30 mV as shown in the inset (0.2 Hz). Two components of outward currents are present in a representative rabbit MSC. One was gradually activating current like delayed rectifier K^+ current (IK_{DR}) at potentials from −20 to +30 mV, and another with noisy oscillation like Ca^{2+}-activated K^+ current (I_{KCa}) at potentials from +30 to +60 mV. (B) IK_{DR} was recorded in another rabbit MSC with the same voltage protocol as shown in the inset of (A). (C) Inward rectifier K^+ current (I_{Kir}) was recorded in a different rabbit MSC with 300-ms voltage steps from −40 to between −120 and 0 mV (inset).

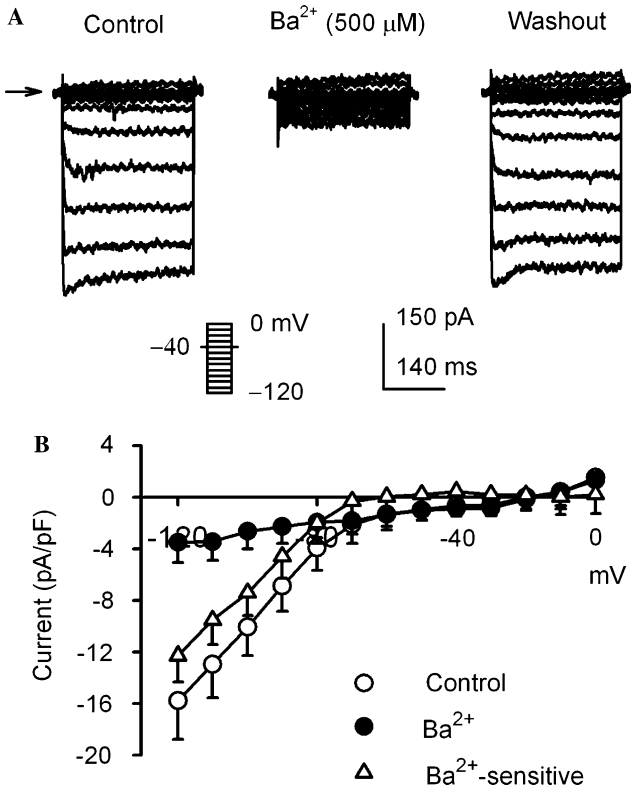

Fig. 2. I_{Kir} in rabbit MSCs. (A) I_{Kir} traces recorded from a representative rabbit MSC during control, in the presence of 500 μM $BaCl_2$, and after washout. The current was elicited with 300-ms voltage steps from −40 to between −120 and 0 mV as shown in the inset. I_{Kir} was reduced by 500 μM $BaCl_2$, and the effect fully recovered upon washout. (B) *I–V* relationships of I_{Kir} during control (open circles), in the presence of 500 μM Ba^{2+} (filled circles), and Ba^{2+}-sensitive current (open triangles) obtained by digital subtraction of current before and after Ba^{2+}. Ba^{2+} significantly inhibited I_{Kir} at −120 to −80 mV ($n = 7$, $P < 0.05$ or $P < 0.01$ vs control).

the Hill equation: $E = E_{max}/[1 + (IC_{50}/C)^b]$, where E is the inhibitory effect of IK_{DR} in percent at concentration C, E_{max} is the maximum inhibition, IC_{50} is the concentration for half-maximum action, and b is the Hill coefficient. The IC_{50} of TEA for inhibiting IK_{DR} was 2.8 ± 0.2 mM with a Hill coefficient of 1.3 ± 0.1 on the basis of cell-by-cell fits. In addition, 4-AP also suppressed IK_{DR} (Fig. 3) and showed a concentration-dependent manner (0.1–10 mM, $n = 8$). The IC_{50} of 4-AP for inhibiting IK_{DR} was 3.2 ± 0.3 mM, and Hill coefficient was 1.4 ± 0.1.

To study properties of IK_{DR}, we analyzed voltage and time dependence of the current recorded in rabbit MSCs without application of any intervention. Fig. 4B displays the *I–V* relationships of IK_{DR} tail current measured at −30 mV and step current measured from the zero current to the end of voltage steps. The current activated at potentials positive to −20 mV and showed a linear *I–V* relation of step current. The tail current reached a steady-state level at +40 and +60 mV. The activation conductance g/g_{max} of IK_{DR} was obtained by normalizing tail current (Fig. 4C) and fitted to Boltzmann distribution [16]. Midpoint ($V_{0.5}$) of IK_{DR} activation was 3.1 ± 0.2 mV, and slope factor was 12.1 ± 0.3 ($n = 15$).

Fig. 4D displays the inactivation process of the current elicited by 4-s voltage steps from −80 to between −10 and +60 mV. Raw data were fitted to mono-exponential functions. The mean values for voltage dependence of inactivation time constant are illustrated in Fig. 4E, showing that inactivation time constant of IK_{DR} increases with the elevation of depolarization potentials ($n = 15$, $P < 0.01$). Fig. 4F displays the voltage protocol and representative recordings used to assess voltage-dependent inactivation (availability) of IK_{DR}. Prepulses of 1- or 4-s were applied to conditioning potentials to pulses of variable potentials followed by a 300-ms test step to +60 mV after a 30-ms interval at −80 mV as shown in the inset. The current was inactivated to maximal at 0 mV (but incompletely even with 4-s conditioning pulses), and rebounded at potentials positive to 0 mV, showing a "U-shaped" inactivation curve with 1- or 4-s

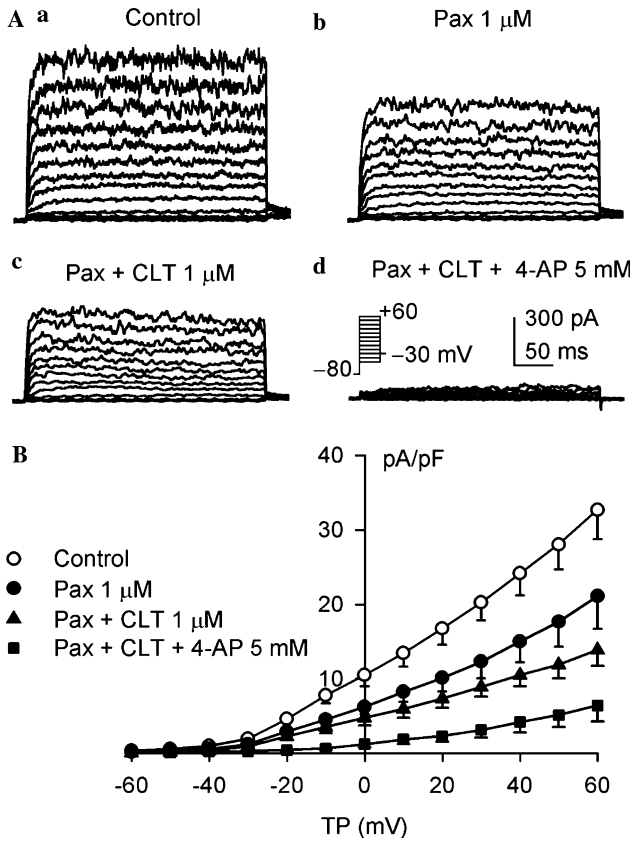

Fig. 3. I_{KCa} in rabbit MSCs. (A) Membrane currents were recorded with the 300-ms voltage steps as shown in the inset under control condition (a), in the presence of 1 μM paxilline (Pax, b), paxilline plus 1 μM clotrimazole (CLT, c), and paxilline with clotrimazole plus 5 mM 4-aminopyridine (4-AP, d). (B) *I–V* relationships during control ($n = 6$), in the presence of 1 μM paxilline ($P < 0.05$ or $P < 0.01$ vs control at −20 to +60 mV), co-presence of paxilline and 1 μM clotrimazole ($P < 0.05$ or 0.01 vs after paxilline), and paxilline plus clotrimazole and 5 mM 4-AP ($P < 0.05$ or $P < 0.01$ vs after paxilline plus clotrimazole).

condition potentials (Fig. 4G), similar to that observed in cloned Kv2.1 channels [22].

Fig. 4H illustrates current traces and voltage protocol used to determine recovery kinetics of IK_{DR} from inactivation. The recovery of IK_{DR} was determined by normalizing the current with P_2 by that with P_1. Fig. 4I shows the mean data of recovery of IK_{DR} from inactivation fitted by a mono-exponential function. On the basis of cell by cell fits, the recovery time constant of IK_{DR} was 1089.7 ± 41.2 ms ($n = 14$).

Messenger RNA expression of functional ion channels

To study molecular identities of the functional ionic channels observed, we examined gene expression of various channels in rabbit MSCs with RT-PCR using the specific primers as shown in Table 1. Fig. 5A displays mRNA expression for α-subunits of ion channels related to functional currents. KCa1.1 and KCa3.1 (possibly responsible for I_{KCa}), Kv1.2, Kv2.1, and Kv2.2 (possibly responsible for IK_{DR}), and Kir1.1 (possibly responsible for I_{Kir}) were detected in rabbit MSCs. In addition, significant mRNA for Kv4.3, $Na_V1.1$, and $Ca_V1.2$ was detected, although functional transient outward K^+ current (I_{to}), Na^+ current (I_{Na}), and L-type Ca^{2+} current ($I_{Ca.L}$) was not observed. The expression of these genes was not observed when RNA was directly used for PCR without RT product (Fig. 5B), suggesting that the genes detected were not from false-positive signals from the contamination of genomic DNA. Figs. 5C and D display relative levels of the specific mRNA of ion channels to the housekeeping gene GAPDH.

Discussion

MSCs from bone marrow of different species have been used for a number of years in the investigation of cell therapy and differentiation [1,5,23,24]. However, cellular electrophysiology or ion channel expression has not been well documented. Kawano and colleagues [15,25] first demonstrated ionic homogeneity in human MSCs, and found that Ca^{2+} oscillations regulated by Na^+–Ca^{2+} exchanger and plasma membrane Ca^{2+} pump might induce fluctuations of membrane current and potentials in human MSCs. In addition, they found that I_{KCa} was present in most of the cells, and nifedipine-sensitive $I_{Ca.L}$ was detected in a small population of human MSCs [15]. The evidence for the expression of big conductance of I_{KCa} and $I_{Ca.L}$ in human MSCs was further supported by Heubach and colleagues [13]. Our study demonstrated that besides I_{KCa} and $I_{Ca.L}$, three more functional ionic channel currents (i.e., I_{to}, $I_{Na.TTX}$, and IK_{DR}) were present in undifferentiated human MSCs [14]. Moreover, we recently studied ion channel properties in rat MSCs, and found that ion channel expression was not identical to that in human MSCs. Although $I_{Na.TTX}$, $I_{Ca.L}$, and I_{to} were detected in both human and rat MSCs [14,16], IK_{DR} in rat MSCs was different from that in human MSCs. In addition, big conductance I_{KCa} was present in human MSCs, while intermediate conductance I_{KCa} were heterogeneously present in some rat MSCs, and a small portion of big conductance I_{KCa} existed in a small population of rat MSCs [16].

The present study provided additional information regarding ion channels in rabbit MSCs. Using a hyperpolarization voltage protocol, the inward rectifier K^+ current I_{Kir} was detected in 28% of rabbit MSCs (Fig. 1C), and the current was sensitive to inhibition by Ba^{2+} (Fig. 2). RT-PCR demonstrated that I_{Kir} channel was likely encoded by Kir1.1 in rabbit MSCs (Fig. 5). However, I_{Kir} was not found in human [13,14] or rat [16] MSCs.

Noise-like I_{KCa} was observed in 29% of rabbit MSCs, the current was co-present with IK_{DR} (Figs. 1 and 3). By the use of selective I_{KCa} channel blockers [19–21], we found that I_{KCa} was sensitive to inhibition by the specific big conductance I_{KCa} channel blocker paxilline (or iberiotoxin) and the relatively selective intermediate conductance I_{KCa} inhibitor clotrimazole (Fig. 3), but not to the small conductance I_{KCa} inhibitor apamin, suggesting that both big and intermediate conductance I_{KCa} are present in rabbit MSCs.

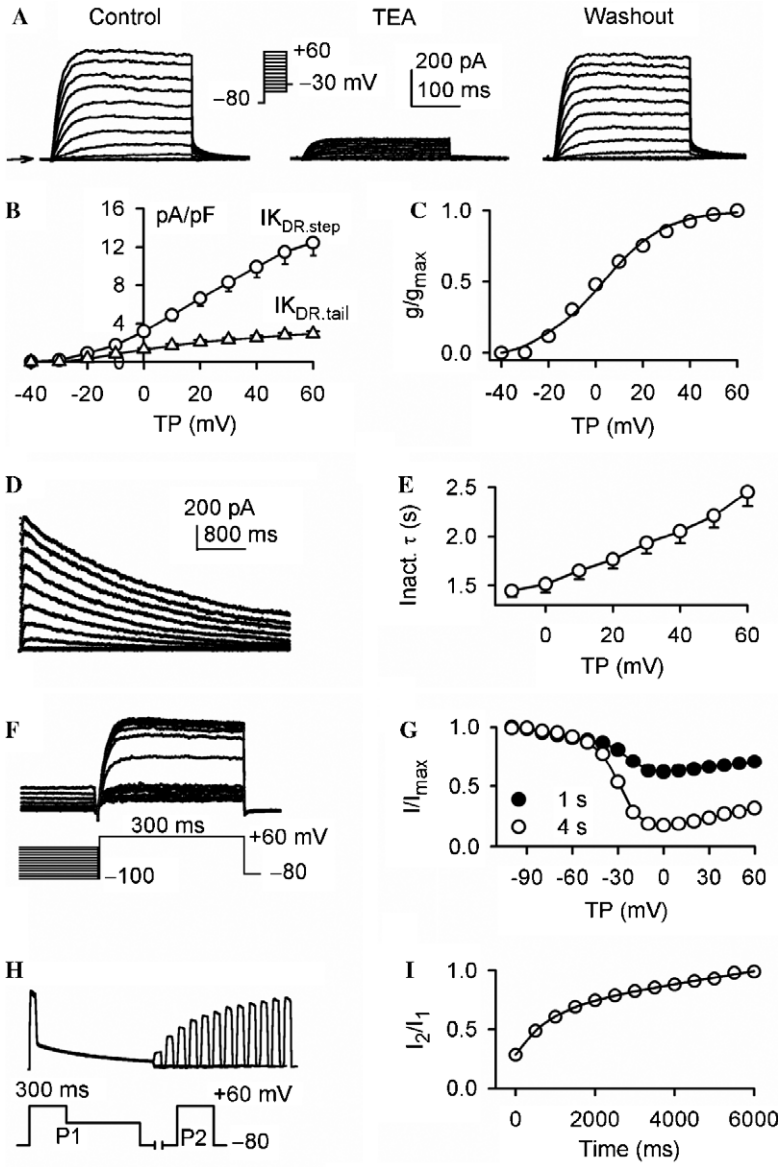

Fig. 4. IK_{DR} in rabbit MSCs. (A) IK_{DR} recorded in a typical experiment with the voltage protocol shown in the inset in the absence and presence of 10 mM TEA. (B) *I–V* relationships of IK_{DR} tail current ($IK_{DR.tail}$) and step current ($IK_{DR.step}$). (C) Activation conductance (g/g_{max}) of IK_{DR} was determined by normalizing $IK_{DR.tail}$ and fitted to Boltzmann distribution: $g/g_{max} = 1/\{1 + \exp[(V_m - V_{0.5})/S]\}$, where V_m is membrane potential, $V_{0.5}$ is the midpoint of IK_{DR} activation, and S is slope factor. The $V_{0.5}$ of IK_{DR} activation was 3.1 ± 0.2 mV, while S was 12.1 ± 0.3 ($n = 15$). (D) IK_{DR} traces recorded from a typical experiment with 4-s depolarization steps to between −10 and +60 mV showing significant inactivation. Raw data were fitted to mono-exponential function. (E) Mean values for voltage dependence of inactivation time constant (Inact. τ) of IK_{DR} ($n = 15$, $P < 0.01$ between test potentials). (F) Protocol and superimposed IK_{DR} traces were used for determining voltage-dependent inactivation (availability) of IK_{DR}. After conditioning potentials (CP, 1 or 4 s) to between −100 to +60 from −80 mV followed by a 30-ms interval potential to −80 mV, IK_{DR} was then determined by a 300-ms test potential from −80 to +60 mV. (G) "U-shaped" availability curves determined by I/I_{max} with 1-s ($n = 15$) or 4-s ($n = 18$) conditioning pulses. (H) Superimposed recordings of IK_{DR} recovery from inactivation obtained with the protocol illustrated in the inset: P1, a 300-ms pulse from −80 to +60 mV, and to 0 mV for 4-s, and then to −80 mV, and P2, a 300-ms pulse from −80 to +60 mV. P1–P2 pulses were delivered at varying P1 and P2 interval every 20 s. (I) Recovery curve was determined by normalizing P2 current by P1 current and plotted against P1–P2 interval. The curve was fitted by mono-exponential functions ($n = 14$).

This notion is supported by the data from RT-PCR. Significant expression levels of KCa1.1 mRNA (possibly responsible for big conductance I_{KCa}) and KCa3.1 mRNA (likely responsible for intermediate conductance I_{KCa}) are found in rabbit MSCs (Fig. 5).

IK_{DR} was activated upon depolarization voltage steps with the activation $V_{0.5}$ of +3.1 mV in rabbit MSCs, and showed significant inactivation with longer depolarization voltage steps, slow recovery from inactivation, and "U-shaped" voltage-dependent inactivation (Fig. 4). These properties were similar to those observed in rat MSC IK_{DR} [16] and cloned Kv2.1 [22]. In addition, RT-PCR revealed significant expression of Kv1.2, Kv2.1, and Kv2.2 mRNA (Fig. 5), suggesting that Kv1.2, Kv2.1, and Kv2.2 likely

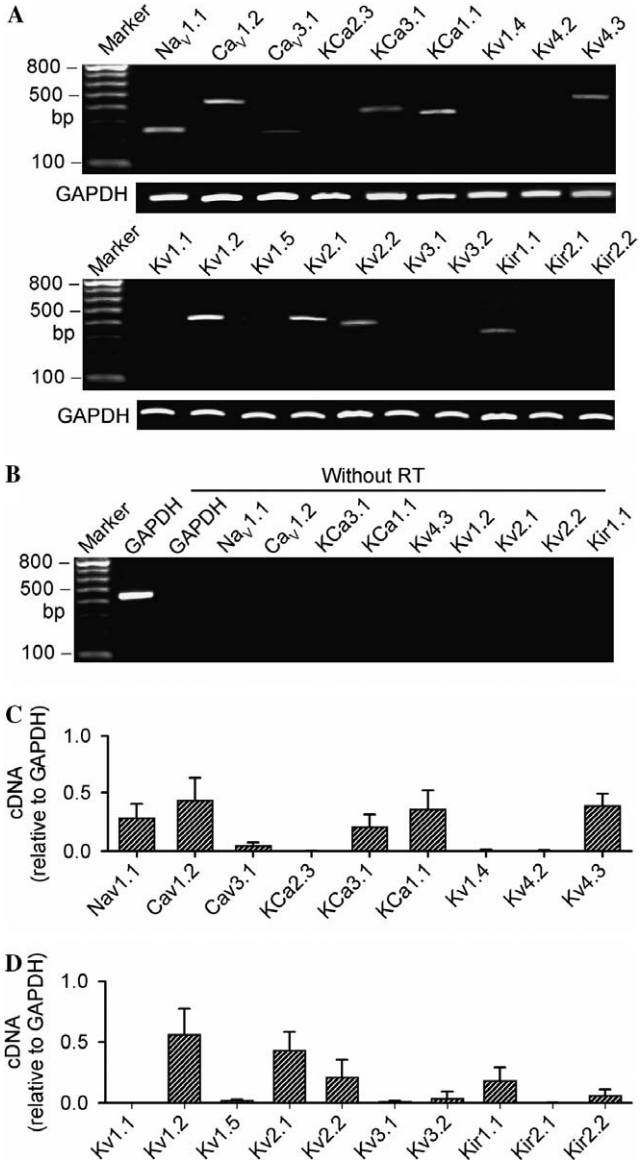

Fig. 5. Messenger RNA (mRNA) of ion channel α-subunits related to the functional ionic currents was amplified by RT-PCR. (A) Original gels showing significant levels of $Na_V1.1$, $Ca_V1.2$, KCa1.1, KCa3.1, Kv4.3, Kv1.2, Kv2.1, Kv2.2, and Kir1.1. (B) The bands for the positive genes as shown in (A) disappeared when RNA was directly amplified by PCR without reverse transcription product. (C,D) Summary of amplification of cDNA derived from mRNA with rabbit MSCs relative to the housekeeping gene glyceraldehyde-3-phosphate dehydrogenase (GAPDH). Significant mRNA expression levels were found for KCa1.1 and KCa3.1 (likely responsible for I_{KCa}), Kv1.2, Kv2.1, and Kv2.2 (likely responsible for IK_{DR}), and Kir1.1 (likely responsible for I_{Kir}). In addition, $Na_V1.1$, $Ca_V1.2$, and Kv4.3 genes were also significant, although functional currents (i.e., I_{Na}, $I_{Ca.L}$, and I_{to}) were not observed ($n = 5$, times of RT-PCR experiments from different cells of 2 to 4 passages as used in ion channel study).

encode IK_{DR} in rabbit MSCs, which is similar to, but not identical to, that in rat MSCs, since IK_{DR} in rat MSCs is not contributed by Kv2.2 [16].

Collectively, multiple ion channels in rabbit MSCs, as in human and rat MSCs, were found in undifferentiated cells. However, types of ion channels and properties of ion channel currents differed in rabbit MSCs from those in human MSCs and/or rat MSCs. First, $I_{Na.TTX}$, $I_{Ca.L}$, and I_{to} were present in a small population of human [14] and rat [16] MSCs, but not in rabbit MSCs, although significant gene expression was detected for I_{Na}, $I_{Ca.L}$, and I_{to} (Fig. 5). Second, both big and intermediate conductance I_{KCa} were found in rabbit MSCs, while only big conductance I_{KCa} was detected in human MSCs, and I_{KCa} was dominantly contributed by the intermediate conductance channel (i.e., KCa3.1) in rat MSCs. Third, properties of IK_{DR} in rabbit MSCs, e.g., remarkable inactivation, "U-shaped" availability, and slow recovery from inactivation (Fig. 4), were similar to those in rat MSCs [16], but were different from those (lack of time- and voltage-dependent inactivation) in human MSCs [14]. The possible molecular base of IK_{DR} was Kv1.2, Kv2.1, and Kv2.2 for rabbit MSCs (Fig. 5), and Kv1.2 and Kv2.1 for rat MSCs [16], whereas heag1 for human MSCs [14]. In addition, I_{Kir} was present in rabbit MSCs, but not in human [13] or rat [16] MSCs. All the differences described above suggest that ion channel expression is species-dependent.

Ion channels are believed to modulate cell cycling in proliferative cells [26]. It was reported that K^+ channel expression changed with cell cycle progression [27], and K^+ channel blockers (e.g., 4-AP, TEA) were anti-proliferative in numerous types of cells such as cancer cells [26,27], T-lymphocyte [28], and vascular smooth muscle cells [19]. Blockade of big conductance Ca^{2+}-activated K^+ channels also inhibited cell proliferation in endothelial cells [29]. Moreover, I_{Kir} was found to participate in the proliferation of astrocytes [27] and hematopoietic progenitor cells [30]. Whether and how ion channels regulate cell proliferation remains to be studied in MSCs from human and animal species.

Expression of the ion channel currents in individual rabbit MSCs, as observed in human [13,14] and rat [16] MSCs, is inhomogeneous. Possible reasons of this heterogeneity may be related to the fact that the cells investigated are not from a homogeneous population of rabbit MSCs, e.g., cells at different phases of the cell cycle [27,31]. Fractions of more or less committed progenitor cells might also affect the expression pattern of ion channels [13,32]. The related mechanisms underlying heterogeneous expression in rabbit MSCs remain to be studied in the future.

Cell transplantation is believed to be a promising treatment strategy for myocardial regeneration. MSCs have been currently used as a cell source for this purpose in experiments with mice [33], rats [12,34], rabbits [35], pigs [36,37], and humans [11,38,39]. However, studies that have raised concern as to whether observed arrhythmic events are a consequence of the intervention or the natural history of underlying disease [40,41]. The present observation focused on the study of ion channel expression, and demonstrated that multiple ion channels were present in rabbit MSCs. The results from the present study and previous reports [13–16] provide a base for understanding of ion channel expression in undifferentiated MSCs from rabbits,

rats, and humans, which will be helpful in seeking possible biological solutions for these concerns and medical challenges.

In summary, the present study demonstrates for the first time that three types of functional ion channels are present in undifferentiated rabbit MSCs, including I_{Kir}, I_{KCa}, and IK_{DR}. The information obtained from the present study provides a basis for investigating how these functional ion channels regulate biological and physiological activity of MSCs in the future.

Acknowledgments

The present study was supported by a RGC grant (HKU 7347/03M) from Research Grant Council of Hong Kong. The authors thank Professor T.M. Wong in the Department of Physiology for his support in the experimental facilities, and Genome Research Centre, the University of Hong Kong for the synthesis of oligonucleotide primers.

References

[1] A.I. Caplan, S.P. Bruder, Mesenchymal stem cells: building blocks for molecular medicine in the 21st century, Trends Mol. Med. 7 (2001) 259–264.
[2] Y. Jiang, B.N. Jahagirdar, R.L. Reinhardt, R.E. Schwartz, C.D. Keene, X.R. Ortiz-Gonzalez, M. Reyes, T. Lenvik, T. Lund, M. Blackstad, J. Du, S. Aldrich, A. Lisberg, W.C. Low, D.A. Largaespada, C.M. Verfaillie, Pluripotency of mesenchymal stem cells derived from adult marrow, Nature 418 (2002) 41–49.
[3] M.F. Pittenger, A.M. Mackay, S.C. Beck, R.K. Jaiswal, R. Douglas, J.D. Mosca, M.A. Moorman, D.W. Simonetti, S. Craig, D.R. Marshak, Multilineage potential of adult human mesenchymal stem cells, Science 284 (1999) 143–147.
[4] M. Reyes, A. Dudek, B. Jahagirdar, L. Koodie, P.H. Marker, C.M. Verfaillie, Origin of endothelial progenitors in human postnatal bone marrow, J. Clin. Invest. 109 (2002) 337–346.
[5] R.J. Deans, A.B. Moseley, Mesenchymal stem cells: biology and potential clinical uses, Exp. Hematol. 28 (2000) 875–884.
[6] L.R. Zhao, W.M. Duan, M. Reyes, C.D. Keene, C.M. Verfaillie, W.C. Low, Human bone marrow stem cells exhibit neural phenotypes and ameliorate neurological deficits after grafting into the ischemic brain of rats, Exp. Neurol. 174 (2002) 11–20.
[7] M. Reyes, T. Lund, T. Lenvik, D. Aguiar, L. Koodie, C.M. Verfaillie, Purification and ex vivo expansion of postnatal human marrow mesodermal progenitor cells, Blood 98 (2001) 2615–2625.
[8] D. Orlic, J. Kajstura, S. Chimenti, I. Jakoniuk, S.M. Anderson, B. Li, J. Pickel, R. McKay, B. Nadal-Ginard, D.M. Bodine, A. Leri, P. Anversa, Bone marrow cells regenerate infarcted myocardium, Nature 410 (2001) 701–705.
[9] M. Sussman, Cardiovascular biology. Hearts and bones, Nature 410 (2001) 640–641.
[10] S. Tomita, R.K. Li, R.D. Weisel, D.A. Mickle, E.J. Kim, T. Sakai, Z.Q. Jia, Autologous transplantation of bone marrow cells improves damaged heart function, Circulation 100 (1999) II247–II256.
[11] K.S. Cahill, C. Toma, M.F. Pittenger, P.D. Kessler, B.J. Byrne, Cell therapy in the heart: cell production, transplantation, and applications, Methods Mol. Biol. 219 (2003) 73–81.
[12] M.F. Pittenger, B.J. Martin, Mesenchymal stem cells and their potential as cardiac therapeutics, Circ. Res. 95 (2004) 9–20.
[13] J.F. Heubach, E.M. Graf, J. Leutheuser, M. Bock, B. Balana, I. Zahanich, T. Christ, S. Boxberger, E. Wettwer, U. Ravens, Electrophysiological properties of human mesenchymal stem cells, J. Physiol. 554 (2004) 659–672.
[14] G.R. Li, H. Sun, X. Deng, C.P. Lau, Characterization of ionic currents in human mesenchymal stem cells from bone marrow, Stem Cells 23 (2005) 371–382.
[15] S. Kawano, K. Otsu, S. Shoji, K. Yamagata, M. Hiraoka, Ca(2+) oscillations regulated by Na(+)–Ca(2+) exchanger and plasma membrane Ca(2+) pump induce fluctuations of membrane currents and potentials in human mesenchymal stem cells, Cell Calcium 34 (2003) 145–156.
[16] G.R. Li, X.L. Deng, H. Sun, S.S. Chung, H.F. Tse, C.P. Lau, Ion channels in mesenchymal stem cells from rat bone marrow, Stem Cells 24 (2006) 1519–1528.
[17] M.T. Harris, D.L. Butler, G.P. Boivin, J.B. Florer, E.J. Schantz, R.J. Wenstrup, Mesenchymal stem cells used for rabbit tendon repair can form ectopic bone and express alkaline phosphatase activity in constructs, J. Orthop. Res. 22 (2004) 998–1003.
[18] H.A. Awad, D.L. Butler, G.P. Boivin, F.N. Smith, P. Malaviya, B. Huibregtse, A.I. Caplan, Autologous mesenchymal stem cell-mediated repair of tendon, Tissue Eng. 5 (1999) 267–277.
[19] R. Kohler, H. Wulff, I. Eichler, M. Kneifel, D. Neumann, A. Knorr, I. Grgic, D. Kampfe, H. Si, J. Wibawa, R. Real, K. Borner, S. Brakemeier, H.D. Orzechowski, H.P. Reusch, M. Paul, K.G. Chandy, J. Hoyer, Blockade of the intermediate-conductance calcium-activated potassium channel as a new therapeutic strategy for restenosis, Circulation 108 (2003) 1119–1125.
[20] B.S. Jensen, M. Hertz, P. Christophersen, L.S. Madsen, The Ca^{2+}-activated K^+ channel of intermediate conductance:a possible target for immune suppression, Expert Opin. Ther. Targets 6 (2002) 623–636.
[21] J. Alvarez, M. Montero, J. Garcia-Sancho, High affinity inhibition of Ca(2+)-dependent K^+ channels by cytochrome P-450 inhibitors, J. Biol. Chem. 267 (1992) 11789–11793.
[22] K.G. Klemic, C.C. Shieh, G.E. Kirsch, S.W. Jones, Inactivation of Kv2.1 potassium channels, Biophys. J. 74 (1998) 1779–1789.
[23] S.P. Bruder, N. Jaiswal, S.E. Haynesworth, Growth kinetics, self-renewal, and the osteogenic potential of purified human mesenchymal stem cells during extensive subcultivation and following cryopreservation, J. Cell. Biochem. 64 (1997) 278–294.
[24] L. Janderova, M. McNeil, A.N. Murrell, R.L. Mynatt, S.R. Smith, Human mesenchymal stem cells as an in vitro model for human adipogenesis, Obes. Res. 11 (2003) 65–74.
[25] S. Kawano, S. Shoji, S. Ichinose, K. Yamagata, M. Tagami, M. Hiraoka, Characterization of Ca(2+) signaling pathways in human mesenchymal stem cells, Cell Calcium 32 (2002) 165–174.
[26] W.F. Wonderlin, J.S. Strobl, Potassium channels, proliferation and G1 progression, J. Membr. Biol. 154 (1996) 91–107.
[27] S.N. MacFarlane, H. Sontheimer, Changes in ion channel expression accompany cell cycle progression of spinal cord astrocytes, Glia 30 (2000) 39–48.
[28] R.K. Rader, L.E. Kahn, G.D. Anderson, C.L. Martin, K.S. Chinn, S.A. Gregory, T cell activation is regulated by voltage-dependent and calcium-activated potassium channels, J. Immunol. 156 (1996) 1425–1430.
[29] J. Wiecha, B. Munz, Y. Wu, T. Noll, H. Tillmanns, B. Waldecker, Blockade of Ca^{2+}-activated K^+ channels inhibits proliferation of human endothelial cells induced by basic fibroblast growth factor, J. Vasc. Res. 35 (1998) 363–371.
[30] O. Shirihai, B. Attali, D. Dagan, S. Merchav, Expression of two inward rectifier potassium channels is essential for differentiation of primitive human hematopoietic progenitor cells, J. Cell. Physiol. 177 (1998) 197–205.
[31] A. Czarnecki, L. Dufy-Barbe, S. Huet, M.F. Odessa, L. Bresson-Bepoldin, Potassium channel expression level is dependent on the proliferation state in the GH3 pituitary cell line, Am. J. Physiol. Cell Physiol. 284 (2003) C1054–C1064.
[32] A. Muraglia, R. Cancedda, R. Quarto, Clonal mesenchymal progenitors from human bone marrow differentiate in vitro according to a hierarchical model, J. Cell Sci. 113 (2000) 1161–1166.

[33] H. Kawada, J. Fujita, K. Kinjo, Y. Matsuzaki, M. Tsuma, H. Miyatake, Y. Muguruma, K. Tsuboi, Y. Itabashi, Y. Ikeda, S. Ogawa, H. Okano, T. Hotta, K. Ando, K. Fukuda, Nonhematopoietic mesenchymal stem cells can be mobilized and differentiate into cardiomyocytes after myocardial infarction, Blood 104 (2004) 3581–3587.

[34] W. Dai, S.L. Hale, B.J. Martin, J.Q. Kuang, J.S. Dow, L.E. Wold, R.A. Kloner, Allogeneic mesenchymal stem cell transplantation in postinfarcted rat myocardium: short- and long-term effects, Circulation 112 (2005) 214–223.

[35] R.B. Thompson, E.J. van den Bos, B.H. Davis, Y. Morimoto, D. Craig, B.S. Sutton, D.D. Glower, D.A. Taylor, Intracardiac transplantation of a mixed population of bone marrow cells improves both regional systolic contractility and diastolic relaxation, J. Heart Lung Transplant. 24 (2005) 205–214.

[36] J.G. Shake, P.J. Gruber, W.A. Baumgartner, G. Senechal, J. Meyers, J.M. Redmond, M.F. Pittenger, B.J. Martin, Mesenchymal stem cell implantation in a swine myocardial infarct model: engraftment and functional effects, Ann. Thorac. Surg. 73 (2002) 1919–1925.

[37] M.J. Price, C.C. Chou, M. Frantzen, T. Miyamoto, S. Kar, S. Lee, P.K. Shah, B.J. Martin, M. Lill, J.S. Forrester, P.S. Chen, R.R. Makkar, Intravenous mesenchymal stem cell therapy early after reperfused acute myocardial infarction improves left ventricular function and alters electrophysiologic properties, Int. J. Cardiol. (2006) in press.

[38] S.L. Beeres, D.E. Atsma, A. van der Laarse, D.A. Pijnappels, J. van Tuyn, W.E. Fibbe, A.A. de Vries, D.L. Ypey, E.E. van der Wall, M.J. Schalij, Human adult bone marrow mesenchymal stem cells repair experimental conduction block in rat cardiomyocyte cultures, J. Am. Coll. Cardiol. 46 (2005) 1943–1952.

[39] A. Blatt, G. Cotter, M. Leitman, R. Krakover, E. Kaluski, O. Milo-Cotter, I.B. Resnick, S. Samuel, D. Gozal, Z. Vered, S. Slavin, M.Y. Shapira, Intracoronary administration of autologous bone marrow mononuclear cells after induction of short ischemia is safe and may improve hibernation and ischemia in patients with ischemic cardiomyopathy, Am. Heart J. 150 (2005) 986.

[40] N.S. Peters, Arrhythmias after cell transplantation for myocardial regeneration: natural history or result of the intervention? J. Cardiovasc. Electrophysiol. 16 (2005) 1255–1257.

[41] Y.M. Zhang, C. Hartzell, M. Narlow, S.C. Dudley Jr., Stem cell-derived cardiomyocytes demonstrate arrhythmic potential, Circulation 106 (2002) 1294–1299.